

Molecular rolling friction: the cogwheel model

O M Braun^{1,2} and Erio Tosatti^{2,3,4}

¹ Institute of Physics, National Academy of Sciences of Ukraine, 03028 Kiev, Ukraine

² International School for Advanced Studies (SISSA), Via Beirut 2-4, I-34014 Trieste, Italy

³ CNR-INFM Democritos National Simulation Center, Via Beirut 2-4, I-34014 Trieste, Italy

⁴ International Centre for Theoretical Physics (ICTP), P.O. Box 586, I-34014 Trieste, Italy

E-mail: obraun@iop.kiev.ua (O.M.Braun)

Abstract. With the help of a two-dimensional model we study rolling lubrication by circular (“2D fullerenes”) molecules for a wide range of parameters. The conditions under which microscopic rolling friction may be effective are identified, and related to the relative ingraining between substrate and molecule, the latter behaving as a nanosized cogwheel.

PACS numbers: 68.35.Af, 81.40.Pq, 61.48.+c, 68.60.-p

Keywords: molecular rolling friction; fullerenes

Submitted to: *J. Phys.: Condens. Matter*

1. Introduction

Feynman [1] famously foreshadowed atomic-scale machines that could perform similarly to their macroscopic analogs. Nowadays the problem of designing nanomechanical devices, in particular, to reduce friction by means of nano- and micro-bearings [2] is real. The possible use of fullerene C₆₀ for molecular nanobearings gave rise to Molecular Dynamics (MD) modeling [3, 4, 5, 6]. Other fullerene-like metal dichalcogenide MX₂ (where M=Mo or W and X=S or Se) molecules were considered as additives in oil lubricants, and predicted to provide interesting tribological properties (e.g., see [7] and references therein). Simulations showed that ball-shaped molecules may either slide or rotate over a surface, depending on the substrate and the position of the molecule. For example, C₆₀ slides on graphite in the AB configuration (hexagonal C₆₀ ring lying flat on graphite), but rotates in the on-top frustrated AB configuration where one C₆₀ corner atom faces the center of the graphite hexagon. The rolling configuration is characterized by very low friction [3, 5], with a predicted friction coefficient of the order $\mu \sim 0.01 - 0.02$ [4] or even smaller [5].

Attempts to realize these ideas experimentally had only limited success so far. A single C_{60} molecule confined between two solid substrates may begin to roll when a torque of order 10^{-19} Nm is applied [8]. However, C_{60} molecules actually condense to form close-packed layers, as found, e.g., on a graphite substrate [9, 10]. A single C_{60} monolayer (ML) takes a crystalline structure with 2D spatial order at low temperatures. It undergoes a first-order orientational order-disorder transition at $T = T_m \approx 260$ K [11], the molecules exhibiting free rotation at $T > T_m$. At T_m there is an abrupt change in friction [12], but the lowest friction coefficient is of order $\mu \sim 0.15$ [10, 12], worse than with traditional oil-based lubricants. Coffey and Krim [13] reported a quartz crystal microbalance study of one or two C_{60} monolayers adsorbed on Ag(111) or Cu(111). There are no rotations in a C_{60} ML on Cu(111), and only a slow change of molecular orientations in the C_{60} /Ag(111) ML. For two ML instead, C_{60} molecules in the second layer rotate freely at 300 K. However a molecularly thin methanol film deposited over the C_{60} , failed to show either the expected low friction, or any essential difference between these systems. Thus this particular nanobearing design apparently would not work.

Some charge transfer and bonding between C_{60} and the metal substrate may be held responsible for hindering the rolling. Another reason lies in the full layer coverage. Balls in macroscopic bearings are arranged so as to prevent contact, but rolling molecules in the ML are always in contact, hindering their mutual rolling and jamming the same way two ingrained rolling cogwheels would. As discussed earlier on [14], a way to avoid jamming is to lower dramatically the coverage, well below one ML (the molecule density should anyway be sufficient to prevent the two surfaces from touching). In view of that, and in the lack of well defined low coverage experiments, a study of the single molecule rolling friction represents a natural starting point, and indeed a revealing one.

Macroscopically, the main source of rolling friction of a ball or tire comes from deformation. Both substrate and roller are (elastically or plastically) deformed at the contact. The deformation energy is partly released and lost as bulk frictional heat when the roller moves on [15]. By designing the bulk so that dissipation is poor, rolling friction can be made 10^2 to 10^3 times lower than the sliding friction; the latter being due to adhesion, i.e., breaking and re-forming of slider-substrate bonds. In the previous work [14] we studied molecular rolling friction for the system, where the lubricant and both substrates were constructed of the same molecules, so that the lubricant and substrates were deformable and commensurate. The minimal friction coefficient found in simulation, was of order $\mu > 0.15$ in agreement with available experimental data. Naturally it emerges a question, what would be a value of μ for the rigid substrates, when the losses due to deformation are absent, or for the case of incommensurate lubricant/substrate interface. As the roller size is decreased however, adhesion grows in importance, eventually becoming the main source of friction. To rotate a molecule, one has to break the molecule-substrate bonds from one side of the molecule and create new bonds on the opposite side. Thus, there are no reasons to expect that molecular rolling friction should be much lower than the sliding friction.

Our present goal is to understand what could be the lowest friction coefficient

attainable for molecular rolling and which system parameters might provide it. Besides, we show that a macro- to microworld mapping does work, but one has to choose properly the macroscopic counterpart, which in the present case is a cogwheel. Because we are interested in general trends, we explore a minimal two-dimensional (2D) model, which allows us to span a large number of parameters, and also provides an easier visualization of the processes inside the lubricant.

2. Model

We consider two substrates with lubricant molecules in between, all of them made up of classical point particles (atoms). Atoms can move in the (x, y) plane, where x is the sliding direction and y is perpendicular to the substrates. The substrates, pressed together by a load force $F_l = N_s f_l$, consist of rigid atomic chains of length N_s and equal lattice constant R_s , so that the system size in the sliding direction is $L_x = N_s R_s$ and the total mass of the substrate is $N_s m_s$ (we use periodic boundary condition along x). The bottom rigid substrate is fixed at $x = y = 0$, the top one is free to move in both x and y . The top substrate is driven along x with speed v_s through a spring of elastic constant k_s . The spring force F , whose maximum value before motion measures the static friction force F_s , and whose average during smooth motion $F_k = \langle F \rangle$ is the kinetic friction force, is monitored during simulation (throughout the paper we normalize forces per substrate atom $f = F/N_s$). Thus, our model is a 2D variant of a typical experimental setup in tribology [15, 16]. Between the substrates we have circular (“spherical”) lubricant molecules built as in Ref. [14]. Each molecule has one central atom and L atoms on circle of radius $R_m = R_{ll}/2 \sin(\pi/L)$ so that their chord distance is R_{ll} . They are coupled with the central atom, additionally to the 12-6 Lennard-Jones (LJ) potential, by stiff springs of elastic constant K_m , $V_{\text{stab}}(r) = \frac{1}{2} K_m (r - R_{\text{stab}})^2$, where the distance $R_{\text{stab}} = R_m + (12 V_{ll}/K_m R_m) [(R_{ll}/R_m)^6 - (R_{ll}/R_m)^{12}]$ is chosen so that the total potential $V_{\text{LJ}}(r) + V_{\text{stab}}(r)$ is minimum at $r = R_m$. With $K_m = 100$ the resulting stiff molecular shape resisted destruction during the simulations. All atoms interact via the LJ potential $V_{\text{LJ}}(r) = V_{\alpha\alpha'} [(R_{\alpha\alpha'}/r)^{12} - 2(R_{\alpha\alpha'}/r)^6]$, where $\alpha, \alpha' = s$ or l for the substrate or lubricant atoms respectively. Thus, the lubricant-lubricant interaction is described by the parameters V_{ll} and R_{ll} , while the lubricant-substrate interaction, by V_{sl} and R_{sl} (direct interaction between the top and bottom substrates is omitted, as they are not allowed to touch). We use dimensionless units, where $m_s = m_l = 1$, $R_{ll} = 1$, and the energy parameters $V_{\alpha\alpha'}$ takes values around $V_{\alpha\alpha'} \sim 1$.

Because a 2D model cannot reproduce even qualitatively the phonon spectrum of a 3D system, and because frictional kinetics is generally diffusional rather than inertial, we use Langevin equations of motion with Gaussian random forces corresponding to temperature T , and a damping force $f_{\eta,x} = -m \eta(y) \dot{x} - m \eta(Y - y) (\dot{x} - \dot{X})$, where x, y are the atomic coordinates and X, Y are the coordinates of the top substrate (the force $f_{\eta,y}$ is defined in the same way). The viscous damping coefficient is assumed to decrease with the distance from the corresponding substrate, $\eta(y) = \eta_0 [1 - \tanh(y/y_d)]$, where

typically $\eta_0 = 1$ and $y_d \sim 1$.

We present simulation results for molecule friction from $L = 5$ (the simplest circular molecule) up to $L = 13$ and 14 , which may be considered as a 2D version of fullerenes. In fact in the 3D case, the surface area of the spherical molecule is $s = 4\pi R_m^2$. If we put $L_3 = 60$ atoms on the surface, this gives $s \approx L_3 R_{ll}^2$, or $R_m/R_{ll} \approx 2.18$. In 2D, the length of the circle is $2\pi R_m \approx L R_{ll}$, or $L \approx 2\pi R_m/R_{ll}$, which leads to $L \approx 13.7$ for the same ratio R_m/R_{ll} as for 3D fullerenes.

3. Rigid molecule

We first consider a rigid circular molecule, i.e., $V_{ll} = \infty$ and $K_m = \infty$. Let us fix X of the top substrate and seek minimum of the potential energy V by varying the coordinate Y of the top substrate, and the center (x_c, y_c) and the rotation angle ϕ of the molecule. The X dependence of V , (x_c, y_c) , and ϕ defines the adiabatic trajectory, which describes the joint substrate and lubricant motion when infinitely slow. We define the activation energy $E_a = \max[V(X)] - \min[V(X)]$, and the magnitude of the static friction force, approximated as $f_s = \max[dV(X)/dX]$ ($f_s \sim E_a$ in our units).

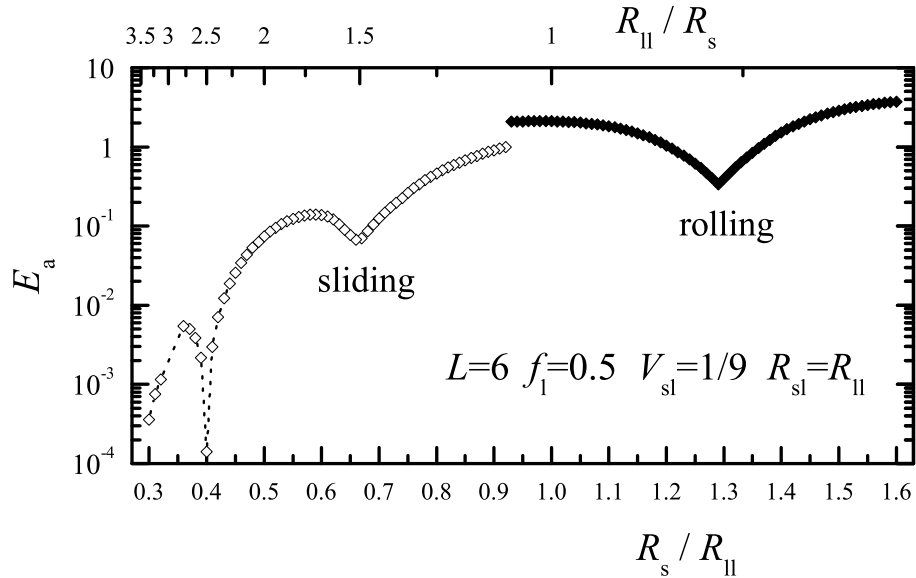


Figure 1. Activation energy E_a as a function of the ratio of the substrate lattice constant R_s to R_{ll} for the rigid $L = 6$ molecule, for $f_l = 0.5$, $V_{sl} = 1/9$, and $R_{sl} = R_{ll}$. Open symbols correspond to sliding, solid symbols to rolling.

Figures 1 and 2 show the results for the $L = 6$ molecule when, to simplify further, R_{sl} is kept constant, $R_{sl} = R_{ll}$. The energy $V(X)$ is periodic with R_s (or a multiplier of R_s). The molecular angle ϕ varies by $\Delta\phi$ as the potential energy $V(X)$ changes from minimum to maximum. Because $\phi(X)$ must be continuous, the motion corresponds to sliding if $\Delta\phi < \phi_0 \equiv 2\pi/L$, while if $\Delta\phi > \phi_0$ the molecule must rotate when it moves. As figure 1 shows, for $R_s < R_{ll}$ the motion corresponds to sliding, i.e., the molecule is

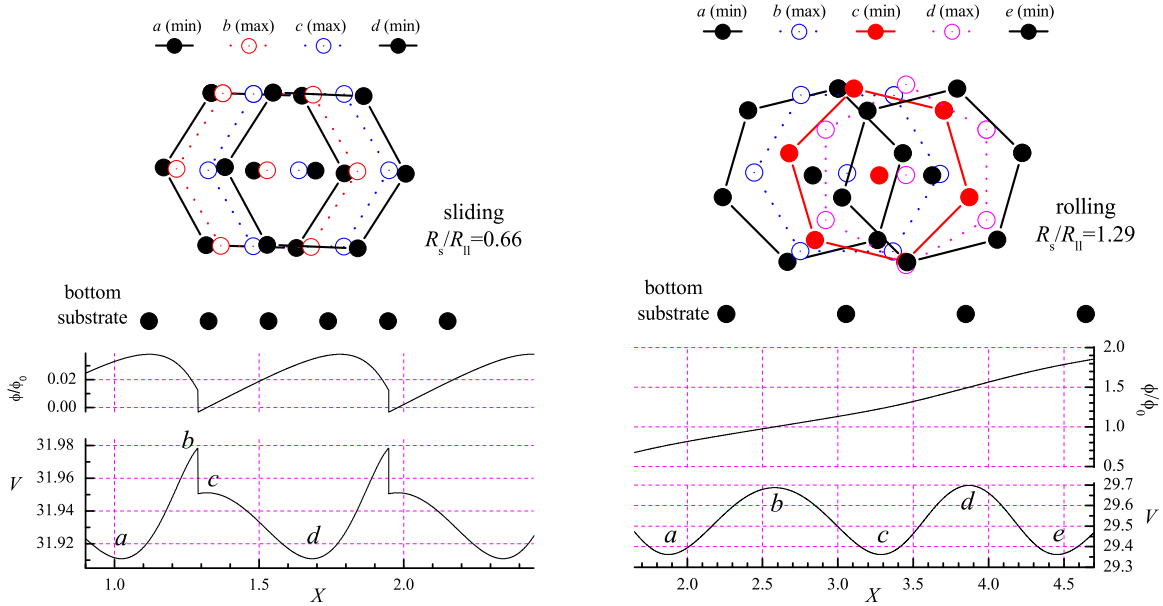


Figure 2. Sliding adiabatic motion of the rigid $L = 6$ molecule for $R_s/R_{ll} = 0.66$ ($\Delta\phi < \phi_0$, left panel) and rolling for $R_s/R_{ll} = 1.29$ ($\Delta\phi > \phi_0$, right panel). Other parameters as in figure 1. Lower panels: X -dependence of potential energy $V(X)$ and the rotation angle $\phi(X)/\phi_0$, where $\phi_0 = 2\pi/L$. Top panel: configurations as the molecule moves from one minimum of $V(X)$ to the next.

shifted as a whole, slightly oscillating during motion (figure 2, left panel). Similarly to the motion of a dimer in a periodic potential [17], the activation energy has maxima at $R_{ll} = nR_s$ (where n is an integer) and minima at $R_{ll} = (n - 1/2)R_s$. On the other hand, for $R_{ll} < R_s$ the motion corresponds to rolling (figure 2, right panel). Here $E_a(R_s)$ has minima at some values of the ratio R_s/R_{ll} (e.g., for $R_s/R_{ll} \approx 1.29$ in figure 1).

Varying R_s in figure 1, we kept fixed the equilibrium distance R_{sl} for the lubricant-substrate interaction. More realistically, it might be reasonable to set, e.g., $R_{sl} = R_s$, in which case, as we observed, the interval of R_s values where rolling prevails is wider than for fixed R_{sl} . Further preference for rolling over sliding is found for increasing load f_l and for decreasing interaction strength V_{sl} . We also note that when sliding wins over rolling for $R_s < R_{ll}$, it provides a lower activation energy. Recalling that $\phi_0 = 2\pi/L$, the region of parameters for rolling should increase with L – a rounder wheel rolls better. The R_s dependence of $E_a(R_s)$ for increasing size L (figure 3) shows rolling for all R_s and for all $L \geq 5$, except for $L = 6$ which shows both rolling and sliding (see open symbols in figure 3a). As R_s varies, the value of E_a changes by more than two orders of magnitude for even L and more than three for odd L , with deep sharp minima separated by broad maxima. Clearly, by suitably choosing R_s/R_{ll} a very strong decrease of rolling friction is attainable.

The deep minima of $E_a(R_s)$ are explained by simple engineering – a “cogwheel model”. Consider the molecule as a cogwheel with L cogs, primitive radius R_m and external radius $R^* = R_m + h$, where $h \propto R_{sl}$. The chord distance between nearest

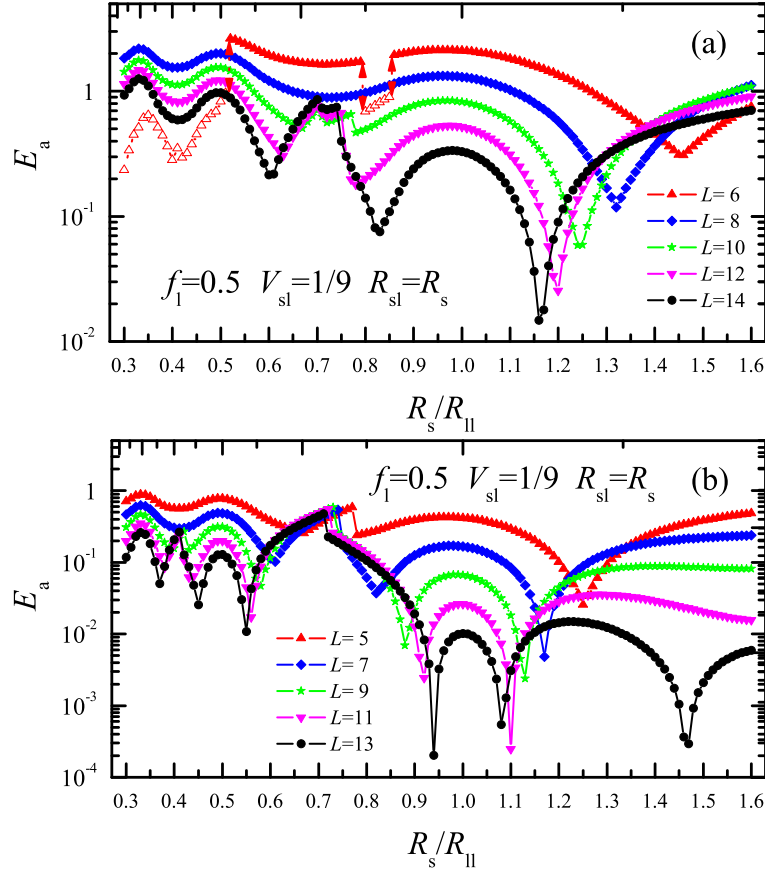


Figure 3. Rigid molecule activation energy E_a versus R_s/R_{ll} for $f_l = 0.5$ and $V_{sl} = 1/9$. Unlike figure 1, here $R_{sl} = R_s$. (a) is for even $L = 6, 8, 10, 12$ and 14 ; (b) is for odd $L = 5, 7, 9, 11$ and 13 . Empty triangles in $L=6$ indicate sliding motion intervals.

cogs is $R_{ll}^* = 2R^* \sin(\pi/L)$. Best rolling conditions are expected when R_{ll}^* matches the substrate potential period R_s , i.e., for $R_s^{(1)} = R_{ll}^*$ and its fractions, $R_s^{(2)} = R_{ll}^*/2$, $R_s^{(3)} = R_{ll}^*/3$, etc. The main minimum of $E_a(R_s)$ is expected at

$$R_s^{(1)}/R_{ll} = 1 + (2h/R_{ll}) \sin(\pi/L). \quad (1)$$

As shown in figure 4, the cogwheel model (1) with $h = \beta R_{sl}$, where β is a parameter, can fit very well the shift of minimum position with molecular size L . It can explain its variation with load (the radius R^* and therefore h decrease as the load grows) as well as with the lubricant-substrate interaction V_{sl} (R^* and h decrease with V_{sl}). It also accounts for the even-odd effect since odd L involves ingraining perfectly one substrate at a time, justifying why roughly double values of β are needed for even relative to odd L .

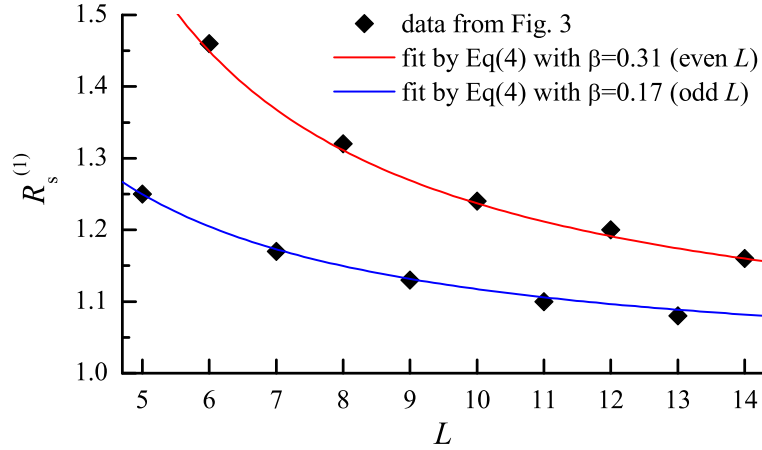


Figure 4. Position $R_s^{(1)}$ of the main minimum of $E_a(R_s)$, extracted from figure 3, for increasing molecular size L . Curves are fits to the cogwheel model (1). The asymptotic limit of 1 is still relatively far for reasonable molecular radii.

4. MD simulation

The simulation results for the static friction of a deformable circular molecule are presented in figure 5. As one could expect, the $L = 3$ or 4 “circular” molecule does

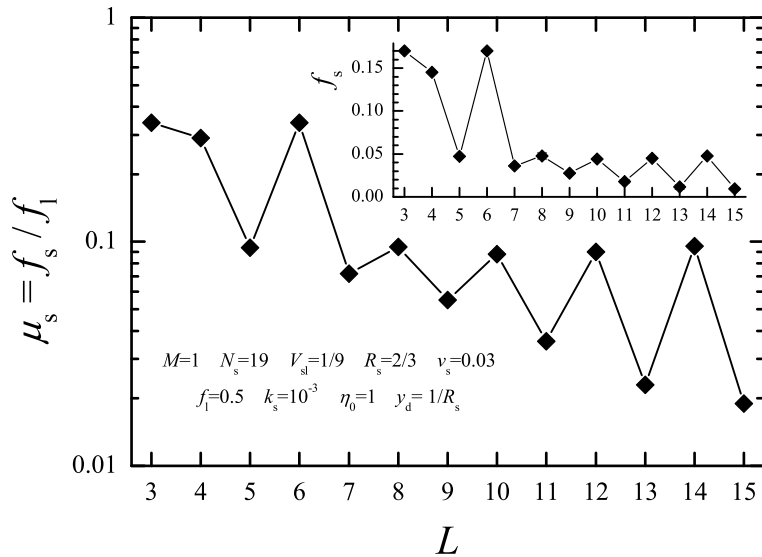


Figure 5. The static friction coefficient $\mu_s = f_s / f_l$ and the friction force f_s (inset) for a single circular molecule as a function of size L . The parameters are $V_{sl} = 1/9$, $R_{sl} = R_s$, $f_l = 0.5$, $N_s = 19$, $R_s = 2/3$, $v_s = 0.03$, $k_s = 10^{-3}$, $\eta_0 = 1$, and $y_d = R_s$.

not roll; instead we observed its “creep” with a relatively large friction. For larger values of L , $L \geq 5$, the molecule may either roll or slide. For rolling in the case of even values of L ($L = 6, 8, 10, 12$ and 14) one needs to break simultaneously two lubricant-substrate bonds (one connecting the lubricant molecule with the bottom substrate, and

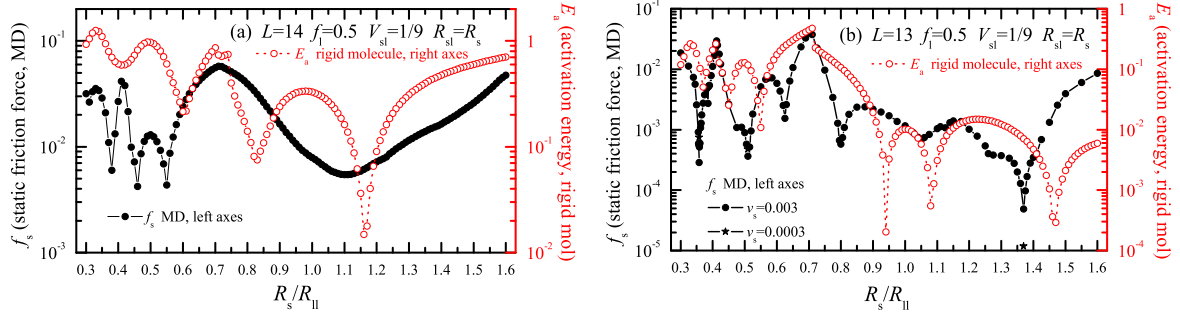


Figure 6. The static friction force f_s for the deformable circular molecule (left axes, $K_m = 100$ and $V_{ll} = 1$, solid curve and circles for $v_s = 0.003$ and stars for $v_s = 0.0003$) and the activation energy E_a for the rigid molecule (right axes, $K_m = \infty$ and $V_{ll} = \infty$, red open symbols and dotted curve) as functions of R_s/R_{ll} for $f_l = 0.5$, $V_{sl} = 1/9$ and $R_{sl} = R_s$. (a) is for $L = 14$, and (b), for $L = 13$.

one, with the top substrate). Therefore, f_s should be approximately independent of L , as indeed is observed in simulation for $L \geq 8$. For odd values of L , $L = 5, 7, 9, 11, 13$ and 15 , f_s is at least two times smaller than for a nearest even L value, because one needs to break one bond only at a time. For all $L \geq 7$ the static friction is relatively low, $\mu_s < 0.1$, and for large odd values the friction may reach quite low values.

The results obtained for the rigid molecules in section 3, are qualitatively confirmed by the static friction force obtained from simulation with deformable molecules. Figure 6 compares the results obtained for the rigid molecule with the MD calculation of the static friction force of the deformable molecule. The agreement between these two dependences is reasonable, at least qualitatively. The friction coefficient $\mu_s = f_s/f_l$ ranges from $\mu_s \sim 0.1$ at $R_s/R_{ll} \sim 0.7$ to $\mu_s \sim 0.01$ or even $\mu_s \sim 0.001$ at $R_s/R_{ll} \sim 1.1$. These results are robust to a change of model parameters. For example, figure 7 compares the dependences $f_s(R_s)$ for two values of the amplitude of lubricant-substrate interaction, $V_{sl} = 1/9$ and $1/3$, and for two values of the load, $f_l = 0.5$ and 0.1 . The next two figures show the dependence of the static and kinetic friction on V_{sl} (figure 8) and on the load (figure 9); the latter demonstrates that the friction force approximately follows the Amontons law

$$f_{s,k} \approx f_{0s,0k} + \mu_{s,k} f_l. \quad (2)$$

Visualization of MD trajectories shows that for $R_s/R_{ll} = 0.7$, where friction is high, rolling rotation is accompanied by a molecular shift/sliding, – much as cogwheels with excessive clearance would do – while for $R_s/R_{ll} = 1.1$, where friction is low, the motion corresponds to pure rotation, corresponding to optimal cogwheel coupling.

Simulations showed that the results presented above remain valid at nonzero temperature T . When T increases, we observed both static and kinetic friction force to decrease, the stick-slip changing to creep and finally to smooth motion at a high temperature. Moreover, we found a transition from stick-slip to smooth rolling for increasing velocity (figure 10). The cogwheel effect remains, and for example calculated

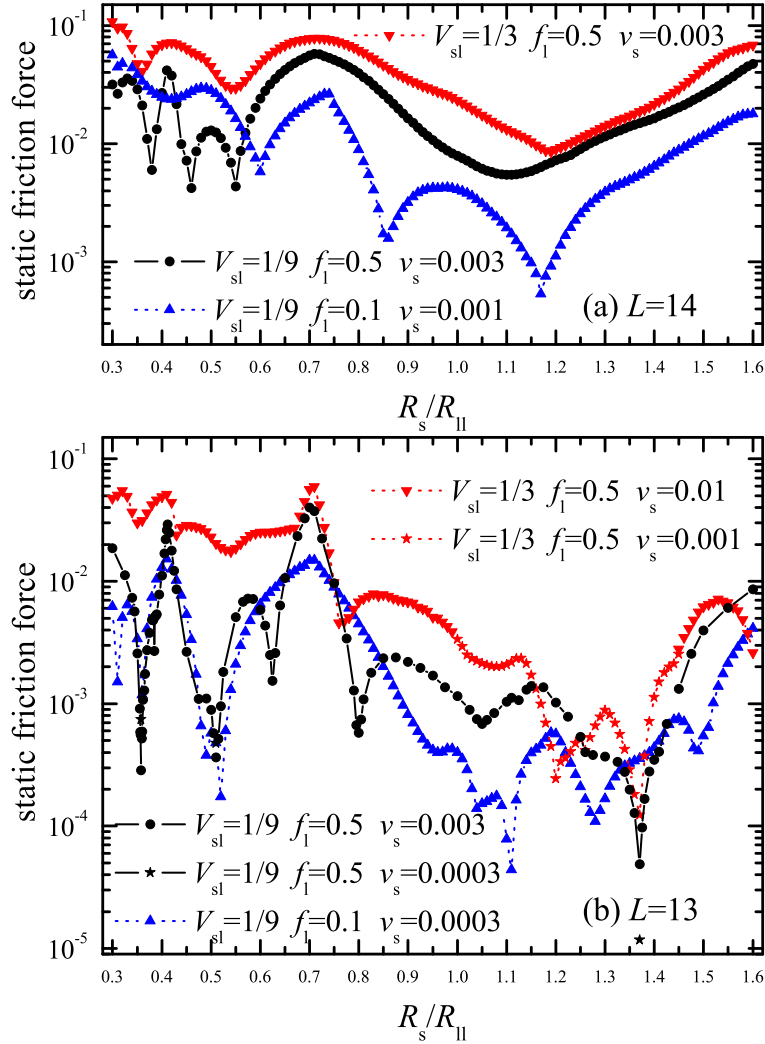


Figure 7. The static friction force f_s as a function of the substrate lattice constant R_s for (a) $L = 14$ and (b) $L = 13$ for different system parameters: (i) $f_l = 0.5$ and $V_{sl} = 1/9$ (solid curve and circles and stars), (ii) $f_l = 0.5$ and $V_{sl} = 1/3$ (down triangles and red dotted curve and stars), and (iii) $f_l = 0.1$ and $V_{sl} = 1/9$ (up triangles and blue dotted curve). Other parameters are $R_{sl} = R_s$, $K_m = 100$, and $V_{ll} = 1$.

static friction for $R_s/R_{ll} = 0.7$ and $R_s/R_{ll} = 1.1$ still differ by a factor of 10 or more. The critical velocity v_c of the transition from stick-slip to smooth rolling also differs by a factor of about four in the two cases. Moreover we always find $f_k \ll f_s$.

The present approach to the single rolling molecule can be extended to a finite coverage of lubricant molecules. For example, figure 11 shows the friction force for a finite concentration of lubricant molecules, which may be compared with those of figure 5 for a single molecule. These results are for approximately the same load per one lubricant molecule ($f_l N_s/M \approx 9.5$ in both cases), and we used a relatively low concentration of lubricant molecules, $M/N_s \approx 0.05$, to avoid jams. The dependence $f_s(L)$ in figure 11 is essentially similar to that of figure 5, although the even-odd oscillation of f_s with

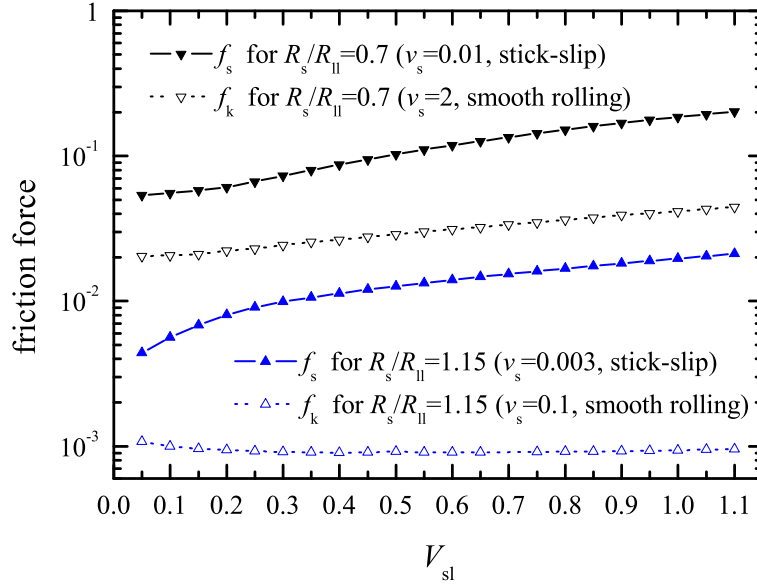


Figure 8. The static friction force f_s (solid curves and symbols, stick-slip motion) and the kinetic friction force f_k (dotted curves and open symbols, smooth rolling) as functions of the amplitude V_{sl} of lubricant-substrate interaction for the deformable $L = 14$ circular molecule for two values of the ratio $R_s/R_{ll} = 0.7$ (down triangles) and $R_s/R_{ll} = 1.15$ (blue up triangles). The parameters are $f_l = 0.5$, $N_s = 19$, $k_s = 10^{-3}$, $\eta_0 = 1$, $y_d = R_s$, $R_{sl} = R_s$, $K_m = 100$, and $V_{ll} = 1$.

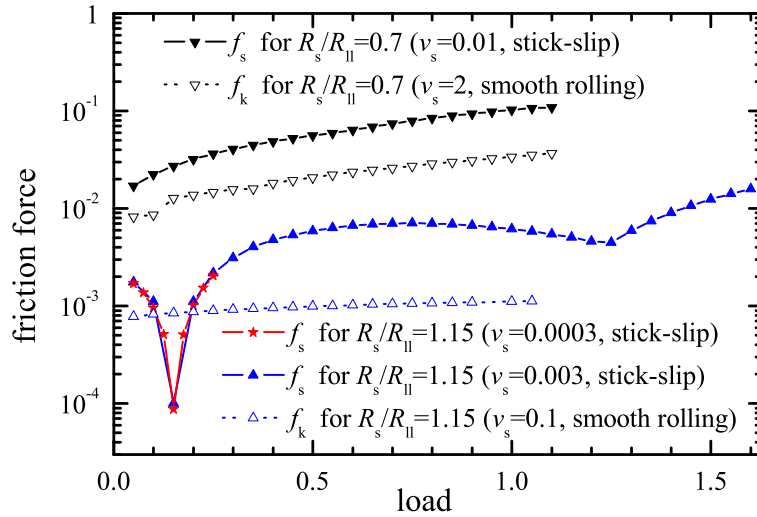


Figure 9. The static friction force f_s (solid curves and symbols, stick-slip motion) and the kinetic friction force f_k (dotted curves and open symbols, smooth rolling) as functions of the load f_l for the deformable $L = 14$ circular molecule for two values of the ratio $R_s/R_{ll} = 0.7$ (down triangles) and $R_s/R_{ll} = 1.15$ (blue up triangles and red stars). The parameters are $V_{sl} = 1/9$, $N_s = 19$, $k_s = 10^{-3}$, $\eta_0 = 1$, $y_d = R_s$, $R_{sl} = R_s$, $K_m = 100$, and $V_{ll} = 1$.

L are less pronounced at the finite concentration because of collisions between the

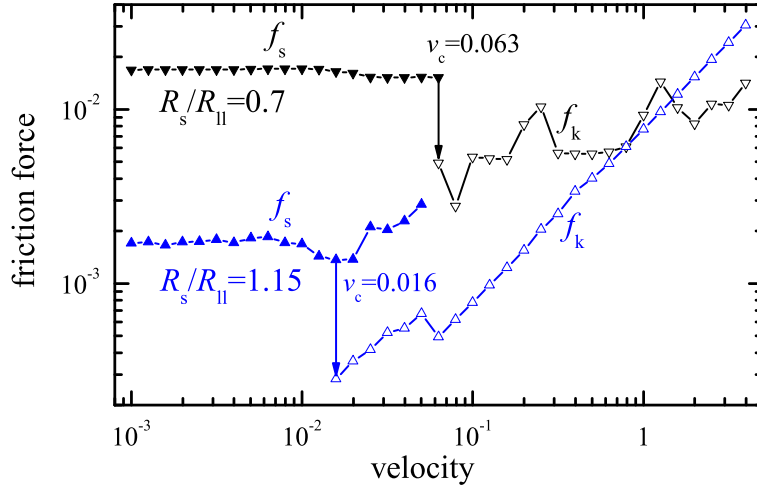


Figure 10. The friction force as a function of the driving velocity v_s for two values of the ratio $R_s/R_{ll} = 0.7$ (down triangles) and $R_s/R_{ll} = 1.1$ (blue up triangles). Solid symbols are for the static friction, open symbols correspond to the kinetic friction; v_c is the critical velocity of the transition from stick-slip to smooth rolling. The parameters are $L = 14$, $f_l = 0.5$, $V_{sl} = 1/9$, $N_s = 19$, $k_s = 10^{-3}$, $\eta_0 = 1$, $y_d = R_s$, $R_{sl} = R_s$, $K_m = 100$, and $V_{ll} = 1$.

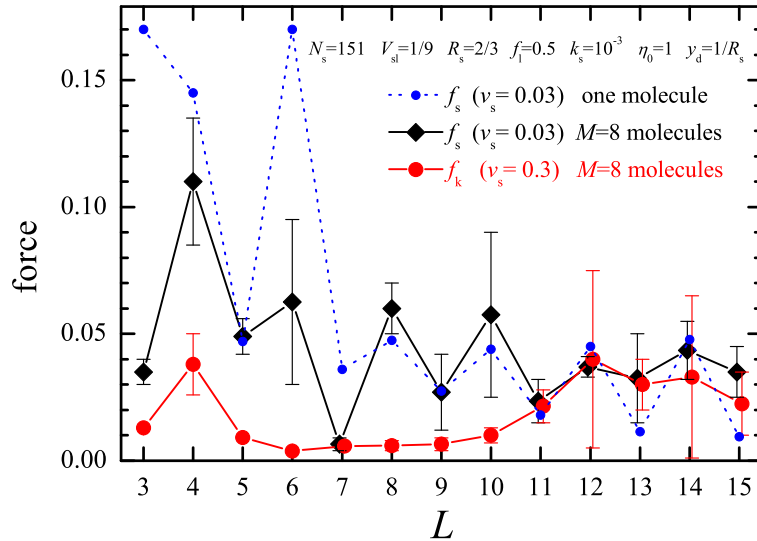


Figure 11. The static (diamonds) and kinetic (red circles) friction force for a finite concentration of circular molecules. The parameters are $N_s = 151$, $f_l = 0.5$, $M = 8$, $v_s = 0.03$ for the static friction (stick-slip) and $v_s = 0.3$ for the kinetic friction (smooth motion); other parameters are as in figure 5. Small blue circles and dotted curve show the results for the single molecule from figure 5.

molecules. As for kinetic friction at high driving velocity $v_s = 0.3$ for smooth motion, it demonstrates a more monotonic behavior with L without even-odd oscillations. The function $f_k(L)$ reaches a minimum at $L = 6$ where $\mu_k < 0.01$, and then increases until $L = 12$; at higher values of L the dependence $f_k(L)$ approximately repeats the behavior

of $f_s(L)$.

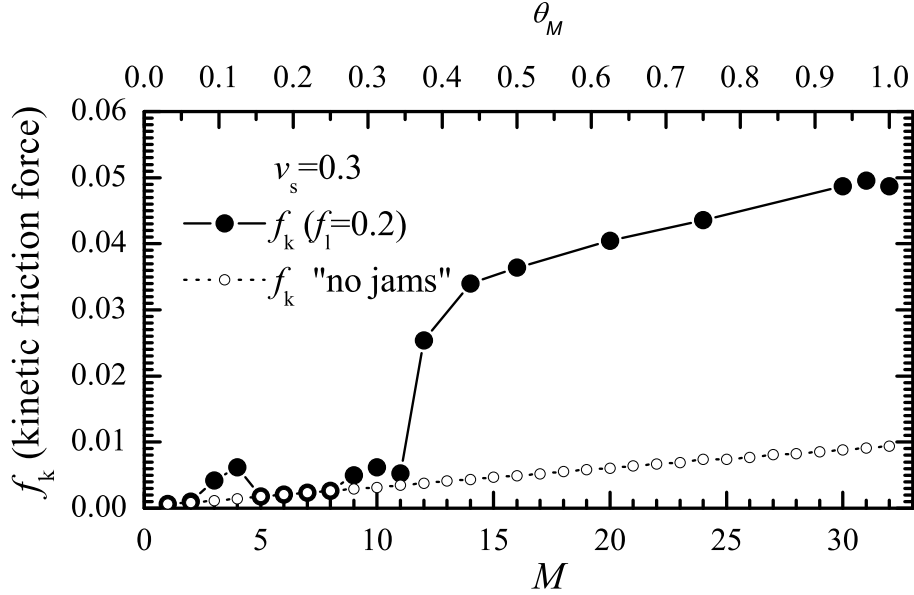


Figure 12. Dependence of the kinetic friction force at $v_s = 0.3$ on the number of circular lubricant molecules M (bottom axes) or on the dimensionless coverage $\theta_M = M/M_1$ (top axes). The parameters are: $L = 14$, $N_s = 151$, $f_l = 0.2$, $R_s/R_{ll} = 1.15$, $V_{sl} = 1/9$, $R_{sl} = R_s$, $k_s = 10^{-3}$, $\eta_0 = 1$, $y_d = R_s$, $K_m = 100$, and $T = 0.05$.

Finally, figure 12 shows the dependence of the friction force on the concentration of lubricant molecules for $L = 14$ and $R_s/R_{ll} = 1.15$, which provided a low friction in the single molecule case (figure 7a). When M increases, the total loading force $F_l = f_l N_s$ is split over the M molecules, so that for a given molecule the load is $f_{l1} = f_l/M$. As the load decreases with M , the friction force per molecule $f_{s1,k1}$ should also decrease according to (2). At the same time, the total friction force should increase, $f_{s,k} = M f_{s1,k1}$. A combined effect is a slow increase of the friction with M as shown in figure 12 with dotted curve and open symbols. In a real situation, coalescence may lead to jamming, with molecules blocking their mutual rotation [14]. In our model, jamming starts already at $\theta_M \approx 0.1$ and completely destroys rolling at $\theta_M > 0.3$ (here $\theta_M = M/M_1$ is the coverage, with M_1 the number of molecules in the monolayer).

5. Conclusion

Summarizing, we can extract from our 2D model the following conclusions. Rolling spherical lubricant molecules can indeed provide better tribological parameters than sliding atomic lubricants. The effect may be as large as in macroscopic friction, where rolling reduces friction by a factor of $10^2 - 10^3$, however *only for sufficiently low coverage of lubricant molecules, and for specially chosen values of the ratio R_s/R_{ll} , corresponding to perfect cogwheel rolling.* To check experimentally these predictions,

it would be interesting to study friction coefficient for different spherical molecules, different coverages, and different substrates. Also, the relative ingraining between the rolling molecule and the substrate may be improved by adjusting the applied load, as it was demonstrated experimentally for the molecular rack-and-pinion device [18]. Inert nonmetal surface (such as perhaps self-assembled monolayers) may represent a better choice of substrate than metals for fullerenes deposition. Because 3D rolling has an azimuthal degree of freedom, the cogwheel effect described should be direction dependent, and rolling friction should exhibit anisotropy depending on direction.

Acknowledgments

This research was supported in part by MIUR PRIN/Cofin Contract No. 2006022847 and by the Central European Initiative (CEI) whose contribution is gratefully acknowledged.

References

- [1] Feynman R P 1960 *Eng. Sci.* **23** 22
- [2] Drexler K E 1992 *Nanosystems: Molecular Machinery, Manufacturing, and Computation* (New York, Wiley)
- [3] Legoas S B, Giro R and Galvão D.S 2004 *Chem. Phys. Lett.* **386** 425
- [4] Kang J W and Hwang H J 2004 *Nanotechnology* **15** 614
- [5] Sasaki N, Itamura N, Tsuda D and Miura K 2007 *Current Nanoscience* **3** 105
- [6] Keeling D L, Humphry M J, Fawcett R H J, Beton P H, Hobbs C and Kantorovich L 2005 *Phys. Rev. Lett.* **94** 146104
- [7] Greenberg R, Halperin G, Etsion I and Tenne R 2004 *Tribol. Lett.* **17** 179
- [8] Miura K, Kamiya S and Sasaki N 2003 *Phys. Rev. Lett.* **90** 55509
- [9] Blau P J and Haberman C E 1992 *Thin Solid Films* **219** 129; Bhushan B, Gupta B K, Cleef Van G W, Capp C, Coe J V 1993 *Appl. Phys. Lett.* **62** 3253; Thundat T, Warmack R J, Ding D, Compton R N 1993 *Appl. Phys. Lett.* **63** 891; Schwarz U D, Allers W, Gensterblum G, Wiesendanger R 1995 *Phys. Rev. B* **52** 14976
- [10] Mate C M 1993 *Wear* **168** 17; Luengo G, *et al.*, 1997 *Chem. Mater.* **9** 1166; Okita S, Ishikawa M and Miura K 1999 *Surf. Sci.* **442** L959; Nakagawa H, Kibi S, Tagawa M, Umeno M, Ohmae N 2000 *Wear* **238** 45
- [11] Heiney P A, Fischer J E, McGhie A R, Romanow W J, Denenstien A M, McCauley Jr. J P and Smith A B 1991 *Phys. Rev. Lett.* **66** 2911; Johnson R D, Yannoni C S, Dorn H C, Salem J R, Bethune D S 1992 *Science* **255** 1235; David W I F, Ibberson R M, Dennis T J S, Hare J P, Prassides K 1992 *Europhys. Lett.* **18** 219
- [12] Liang Qi, Tsui O K C, Xu Y, Li H and Xiao X 2003 *Phys. Rev. Lett.* **90** 146102
- [13] Coffey T and Krim J 2006 *Phys. Rev. Lett.* **96** 186104
- [14] Braun O M 2005 *Phys. Rev. Lett.* **95** 126104
- [15] Persson B N J 1998 *Sliding Friction: Physical Principles and Applications* (Springer-Verlag, Berlin)
- [16] Braun O M and Naumovets A G 2006 *Surf. Sci. Reports* **60** 79
- [17] Braun O M 1990 *Surface Sci.* **230** 262
- [18] Chiaravallotti F, Gross L, Rieder K-H, Stojkovic S M, Gourdon A, Joachim C and Moresco F 2007 *Nature Materials* **6** 30